Cell Communication and Signaling

RESEARCH Open Access

Long non-coding RNA H19 transported by colorectal cancer small extracellular vesicles promotes alternative splicing in healthy hepatocytes: new insights on liver pre-metastatic niche formation

Marco Loria[1,2], Denise Anello[1], Aurora Cordaro[1], Chiara Zichittella[1], Simona Fontana[1], Riccardo Alessandro[1,3] and Alice Conigliaro[1,4*]

Abstract

Colorectal cancer (CRC) is the second most lethal cancer and metastatic dissemination of CRC cells, which predominantly occurs to the liver, is the principal cause of death. Many studies have highlighted the role of CRC-derived small extracellular vesicles (CRC-sEVs) in priming the pre-metastatic niche (PMN) in the liver, promoting morpho-functional alterations which pave the way for the establishment of a favourable microenvironment for future organ colonization by metastatic cells. Our research group demonstrated the effects of CRC-sEVs in promoting the epithelial-to-mesenchymal transition (EMT) of healthy human hepatocytes. In this study, we focused our attention on the long non-coding RNA H19 (lncH19), an oncogenic non-coding RNA whose role in CRC progression has been widely documented. Our data demonstrated that lncH19 is specifically loaded inside CRC-sEVs, carrying with it the RNA binding Fox-1 Homolog 2 (RBFOX2). The treatment of healthy human hepatocytes with CRC-sEVs allows the horizontal transfer of the complex that conveys a pro-EMT post-transcriptional modulation of RBFOX2 target genes.

Keywords Non-coding RNA, Extracellular vesicles, Alternative splicing, Colorectal cancer

*Correspondence:
Alice Conigliaro
alice.conigliaro@unipa.it
[1]Department of Biomedicine Neuroscience and Advanced Diagnostic (Bi.N.D.), University of Palermo, Section of Biology and Genetics, Palermo 90133, Italy
[2]Department of Molecular Medicine, Sapienza University of Rome, Rome, Italy
[3]Institute for Biomedical Research and Innovation (IRIB), National Research Council (CNR), Palermo, Italy
[4]ATeN Center – Advanced Technologies Network Center, University of Palermo, Palermo, Italy

Background

Alternative Splicing (AS) is a crucial post-transcriptional regulatory mechanism that affects over 95% of human genes. Recurrent somatic mutations in components of the human splicing machinery have been observed in human solid and haematological malignancies. These alterations can promote tumorigenesis as oncogenic drivers and/or passengers and may impact proliferation and apoptosis, invasion and metastasis, angiogenesis, and metabolism. Emerging data demonstrated that aberrant splicing events were closely associated with cancer progression, metastasis, therapeutic resistance, and other oncogenic processes [1–4].

In colorectal cancer (CRC), AS is a key feature for transcriptomic variations, likely to be an important determinant of both biological regulation and prognosis of cancer [5, 6]. The inclusion or exclusion of an exon in the mature transcript depends on both cis-regulatory sequences, present in the pre-mRNA, and trans-regulatory molecules, including heterogeneous nuclear ribonucleoproteins (hnRNPs), SR (Serine-Arginine rich) proteins and RBFOX proteinsRBFOX1 and RBFOX2.

RBFOX2 (RNA binding Fox-1 Homolog 2) is the master regulator of tissue-specific alternative splicing, also known to be involved in the development of ovarian and breast cancer, as well as EMT [7, 8]. Depending on both binding site recognition and molecular interactors, RBFOX2 allows exon inclusion or exclusion, and it has also been implicated in the process of microexon splicing, associated with CRC metastasis [9]. Our recent data demonstrated that in CRC, the long non-coding RNA H19 (lncH19) binds the splicing factor RBFOX2 and transports this to specific splicing sites. Explicitly, we demonstrated, both in vitro and in vivo, that lncH19 is required for the RBFOX2-induced AS of the Rho GTPase RAC1, inducing the expression of the constitutively activated RAC1B isoform, whose expression in human colorectal cancer is associated with aggressive disease and poor prognosis [10].

The majority of CRC-related deaths are attributed to metastatic disease, and the liver is the most common site of CRC metastases [11]: up to 25% CRC patients may have synchronous colorectal cancer-liver metastases (CRC-LM) [12, 13]. Metastasising cancer cells show site-specific tropism upon encountering a unique tissue microenvironment to adapt and survive. Since 1889, when Paget proposed the "seed and soil" hypothesis, unravelling how disseminating tumour cells show a selective preference for specific organs and tumour-derived Extracellular Vesicles (TD-EVs) are gaining a prominent role in the ability to "fertilise" the site of metastasis. Mediating cell-cell communication in the surroundings of the primary tumour, such as in distant sites, the TD-EVs promote the establishment of a receptive site for metastatic cells colonisation [14]. The liver represents one of the major "hubs" for disseminating cancer cells [15], and CRC-sEVs can promote the establishment of a favourable pro-metastatic environment.

In a recent manuscript, we demonstrated that CRC-sEVs educated the liver as a metastatic niche by inducing EMT and pro-fibrotic phenotype in healthy hepatocytes [16]. Although the role of vesicles in intercellular communication is now officially recognised, current interest is focused on identifying and characterising the biomolecules that, transported by vesicles, can work within the target cell, inducing phenotypic change.

We were the first to demonstrate that lncH19 can be loaded in TD-EVs released by aggressive hepatocellular carcinoma [17]. Subsequently, other groups detected lncH19 in EVs released by Prostate, Gastric and Breast Cancers, with effects in promoting chemoresistance or, more generally, in tumor progression [18, 19]. In all these cases, the activity of the lncH19 is mainly attributable to its role as a sponge for miRNAs.

Here, we described that CRC-derived EVs also contain the lncH19 and hypothesised its role as a guide for the splicing factor RBFOX2 inside EVs and subsequently in recipient hepatocytes. The data described above indicated that CRC-derived EVs, containing both lncH19 and RBFOX2, induced pro-EMT alternative splicing in healthy hepatocytes (Fig. 1).

Materials and methods

Cell cultures

The colorectal cancer cell lines SW480 (ATCC CCL 228), SW620 (ATCC CCL-227) and HCT-116 (ATCC CCL-247) were used as a source for sEVs. SW480 and SW620 were maintained in RPMI 1640 medium (Euroclone, UK), while HCT-116 was maintained in McCoy's 5 A medium (Euroclone, UK), both supplemented with 10% fetal bovine serum (FBS; Corning), 2 mM l-glutamine (Euroclone, UK), 100 U/ml penicillin, and 100 µg/ml streptomycin (Euroclone, UK). Before use, FBS (South America origin EU approved, Euroclone, UK) was ultracentrifuged for 1 h and 45 min at 100.000 × g in a Type 70 Ti fixed angle rotor to eliminate bovine sEVs.

The SV40 large T antigen-immortalized healthy human liver epithelial cell line THLE2 (ATCC, Manassas, VA) was cultured in Airway Epithelial Cell Basal Medium (ATCC, Manassas, VA) with the Bronchial Epithelial Cell Growth Kit (ATCC PCS-300–040, Manassas, VA) supplemented with 5 ng/ml epidermal growth factor (EGF), 70 ng/ml phosphoethanolamine, 10% fetal bovine serum, 100 U/mL penicillin, and 100 µg/ml streptomycin (Euroclone, UK) at 37 °C with 5% CO_2. THLE2 were cultured in precoated flasks with a collagen coating made of a mixture 0.03 mg/ml bovine collagen type I (Advanced Biomatrix, San Diego region, California, USA), and 0.01 mg/

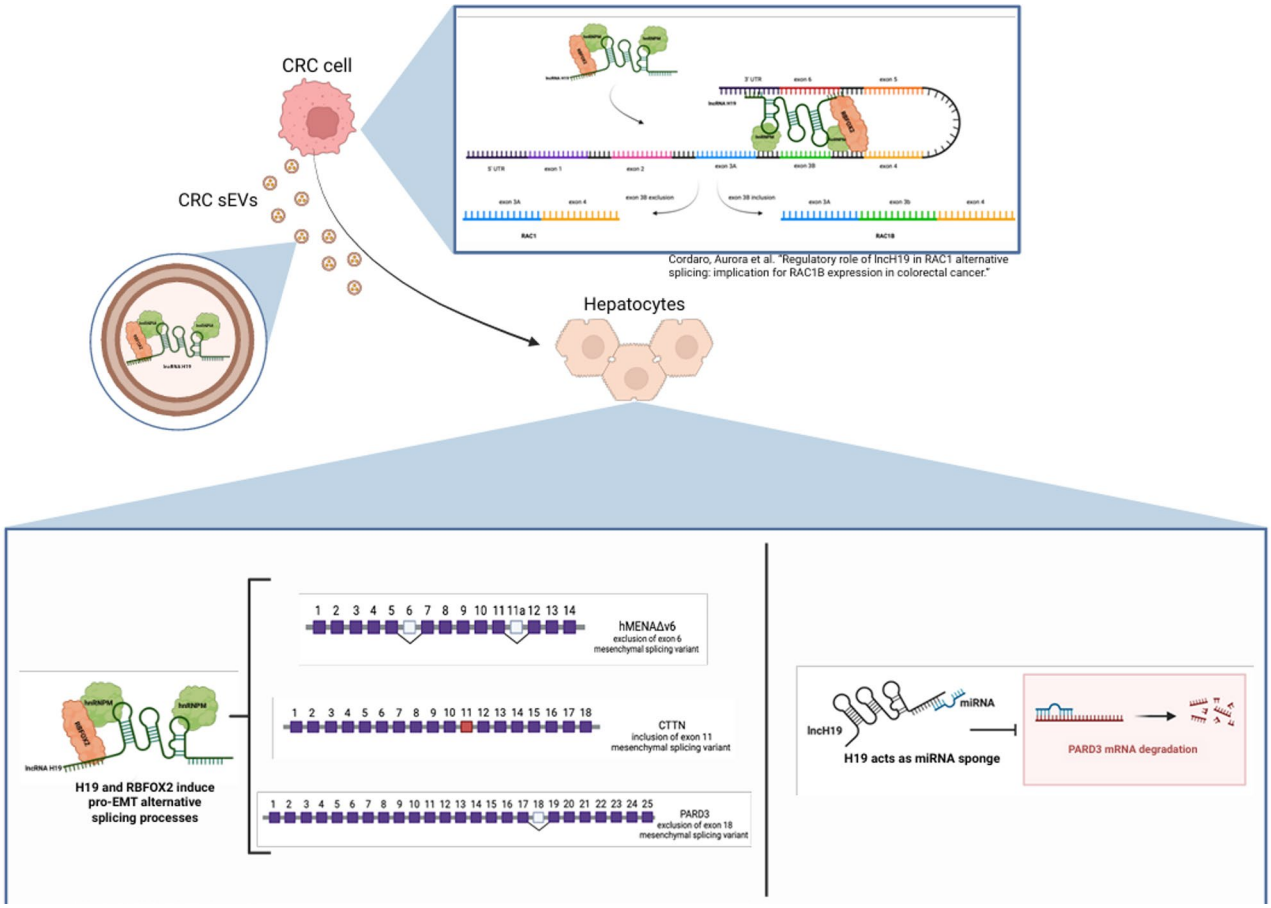

Fig. 1 Schematic representation of the proposed model. LncH19 alongside splicing factors is transported by CRC-sEVs in healthy hepatocytes, where this molecular complex affects gene expression by regulating Alternative Splicing and sponging miRNA target

ml bovine serum albumin (Sigma Aldrich, St Louis, MO, USA). All cell lines were tested for Mycoplasma using Hoechst staining and N-GARDE Mycoplasma PCR reagent set (Euroclone). Moreover, morphology and proliferation rate were constantly evaluated.

Infection with lentiviral vectors to stably silence hnRNPA2/B1 and lncH19

SW480, SW620 and HCT-116 cells were stably silenced for heterogenous nuclear ribonucleoprotein A2/B1 (hnRNPA2/B1) by lentiviral infection with hnRNPA2/B1 lentiviral particles (Cat. n° TL312380VCA OriGene Technologies, Inc., Rockville, MD, United States), relative control cells were infected with control shRNA lentiviral particles (Cat. n° TR30021V, OriGene Technologies, Inc., Rockville, MD, United States). Subsequently, infected cells were selected by cell sorting (BD FACSAria™ III Sorter, ATeN Center) and maintained in culture under selective pressure with 2 µg/ml of puromycin (Gibco™ puromycin dihydrochloride, cat. n°A1113802, Thermo Fisher® Scientific, United States). Silencing efficiency was regularly tested by qRT-PCR and Western Blot, and the fluorescence signal from Green Fluorescent Protein (GFP) expression was frequently observed at Fluorescence Microscopy (Nikon Eclipse Ti).

Extracellular vesicles isolation

SEVs were isolated from the conditioned media of wild-type and silenced cells (SW480, SW620 and HCT-116) cells maintained in the presence of EV-depleted FBS. The conditioned medium was collected after a culture period of 48 h and then subjected to differential centrifugation followed by ultracentrifugation according to the described protocol: the conditioned medium was centrifuged at 4 °C for 5 min at 300 × g, 15 min at 3.000 × g and 30 min at 10.000 × g. The supernatant was then ultracentrifuged at 4 °C for 1 h and 45 min at 100.000 × g in a Type 70 Ti fixed angle rotor. The obtained sEV pellet was resuspended in a range of 60–120 µl PBS, quantified by the Bradford protein assay (Pierce™ Coomassie Plus Assay Kit, cat. n° 23236, Thermo Fisher Scientific, USA) aliquoted and stored at – 80 °C.

Treatment of the THLE2 with the CRC-sEVs

To investigate the effects induced by CRC-sEVs on hepatocytes, the following treatment protocol was performed. After reaching subconfluence, THLE2 cells were treated for the indicated time-points with approximately 1.5*E10 particles of sEVs derived from wt- and sh-SW480, SW620 and HCT-116 cell lines corresponding to 20 µg/ml, a biological dose which was found effective in previous studies [20]. After treatment, the cells were harvested for real-time quantitative PCR, *RNA in situ* or immunofluorescence analysis by confocal microscopy.

RNA isolation and real-time quantitative PCR

Total RNA was extracted using Macherey–Nagel™ NucleoSpin™ miRNA Kit (Cat. n°740971.250, Macherey–Nagel, Germany), according to the manufacturer's instructions. The RNA was reverse transcribed to cDNA using the High-Capacity cDNA Reverse Transcription kit (Cat. n° 4368814, Applied Biosystem™, USA). Then, the cDNA was used to perform quantitative real-time reverse transcriptase-polymerase chain reaction (qRT-PCR) analysis. The sequences of the primers used are reported in Table 1. The qRT-PCR was performed using a Step One™ Real-time PCR System Thermal Cycling Block (Applied Biosystems, Waltham, MA, USA) in a 20 µl reaction containing 300 nM of each primer, 2 µl template cDNA, and 18 µl 2X SYBR Green I Master Mix (Cat. n° 4309155, Applied Biosystems™, USA). The primers' sequences used for expression analysis of the genes of interest are reported in Table 1. Gene expression levels were normalised using β-actin as an endogenous control. Finally, the data are presented as $2^{\wedge -\Delta Ct}$ and $2^{\wedge -\Delta\Delta Ct}$ compared with the untreated control. For lncH19 absolute quantification in CRC-sEVs and CRC cells, known concentrations of lncH19 cDNA plasmid were used for the standard curve (from 1.2 µg to $1.2 * 10^{-11}$ µg).

Table 1 qRT-PCR primers list

Gene	Forward	Reverse
LncH19	TCGTGCAGACAGGGCGACATC	CCAGCTGCCACGTCCTG-TAACC
RbFOX2	CCAGCTTTCAAGCAGATGT-GTCC	CAAATGGGCTCCTCT-GAAAGCG
HnRNPA2/B1	CAGCAACCTTCTAACTACG-GTCC	CACTGCCTCCTGGAC-CATAGTT
ENAH	GACACTTGTCTCCCGTCTCC	TCTGTTCACTCATGGTGCCG
ENAHex6	TGCTGGGAGACTCTTCTGCT	CCTGTTGGGATGGAGTCTCG
ENA-Hex11a	CCAGACGGGATTCTCCAAGG	TTTGGTCTGTGTAATGAAT-CATAGG
CTTN	CCGACCGAGTAGACAAGAGC	GTCGATACCGTATTTGCCGC
CTTNex11	GACAAATGTGCCCTTGGCTG	CTGCCTCTCCGACTGAACAC
PARD3	TTCGCTGTTGAGAAGCACCA	ATCTGCATCTGGCTTGGCTC
PAR-D3ex18	AGCAATTTTCAGATGC-CAGTCA	TTCTGGTCATCCACTGTATT-GAGTT
β-ACTIN	CAAGAGATGGCCACGGCTGCT	TCCTTCTGCATCCTGTCGGCA

THLE2 transfection for lncH19 over expression

THLE2 cells were seeded at 1.5×10^4 in 6-well plates. After 24 h from seeding, cells were transfected with 1.2 µg/ml of H19-pFLAG-CMV-2 expression vector (Cat. n° E7033, Sigma-Aldrich, USA), or empty pFLAG-CMV-2 as Negative Control (Sigma-Aldrich). HiPerFect Transfection Reagent (Cat. n° 301704, Qiagen, Germany) was used following the manufacturer's standard instructions. Eighteen hours after transfection, the cells were processed for the indicated experiments.

Protein lysates preparation and Western blot

Colorectal cancer and THLE2 cells, or sEVs were lysed using RIPA buffer with protease inhibitor cocktail (1:100 dilution, Thermo Fisher Scientific, Waltham, MA, USA) with gentle shaking for 1 h on ice and then centrifuged at 18.800 × g for 15 min at 4 °C. The extracted proteins were quantified through Bradford protein assay (Pierce™ Coomassie Plus Assay Kit, cat. n° 23236, Thermo Fisher Scientific, USA). Protein lysates were separated on Bolt 4–12% Bis–Tris Plus precast polyacrylamide gels (Cat. n° NP0326BOX, Invitrogen by Thermo Fisher Scientific, Waltham, MA, USA) in reducing conditions. After the electrophoresis, proteins were transferred to a nitrocellulose blotting membranes (Amersham Protran Premium 0.45 µm NC by GE HealthCare Life Science, Little Chal font, Buckinghamshire, UK), blocked in 5% Milk Blocking Solution and incubated with primary antibodies overnight at 4 °C with gentle shaking. The following primary antibodies were used for detecting the proteins of interest: anti-RBM9/ RBFOX2 (1:1000 dilution, cat. n° A300-864, A Bethyl Fortis, Montgomery, Texas) and anti-hnRNPA2/B1 (1.1000 dilution, cat. n° PA5-30960, Invitrogen). Primary antibodies used for sEV characterization [21]: were anti-CD81 (1:1000 dilution, Santa Cruz Biotechnology, Dallas, TX, USA), anti-HSC70 (1:1000 dilution, Santa Cruz Biotechnology, Dallas, TX, USA), anti-Calnexin (1:1000 dilution, Santa Cruz Biotechnology, Dallas, TX, USA), anti-cytochrome c (1:1000; Cell Signaling Technology, Danvers, MA, USA) anti-HSP70 (1:1000 dilution, Santa Cruz Biotechnology, Dallas, TX, USA) anti-TSG101(1:1000, Santa Cruz Biotechnology, Dallas, TX, USA). Anti-β actin (1:1000 dilution, Santa Cruz Biotechnology, Dallas, Tx, USA) and anti-Tubulin (1:1000 dilution, Santa Cruz Biotechnology, Dallas, TX, USA), were used for housekeeping proteins used as loading control. Subsequently, membranes were washed with Tris-buffered saline + Tween-20 (TBS/T) three times and incubated with horseradish peroxidase (HRP)-conjugated goat anti-rabbit, anti-mouse or anti-chicken secondary antibodies (1:1000 dilution, Thermo Fisher Scientific, Waltham, MA, USA) at room temperature for 1 h in gentle shaking. Finally, the protein bands were visualised through enhanced chemiluminescence (ECL™ Prime

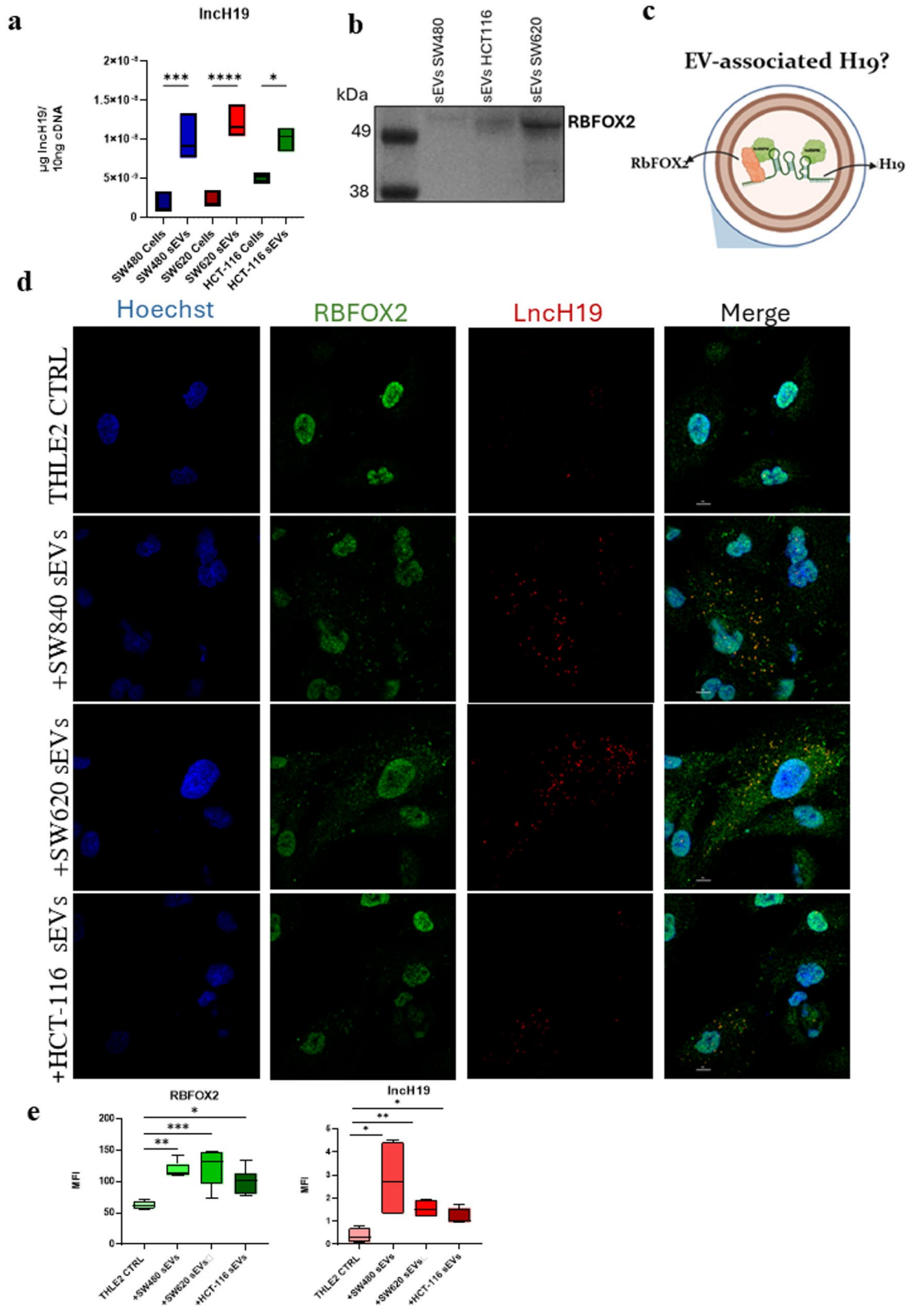

Fig. 2 (See legend on next page.)

(See figure on previous page.)

Fig. 2 **a** qRT-PCR showing lncH19 levels inside CRC-sEVs and CRC_cells. **b** Representative images of western blot for the presence of RBFOX2 in the CRC-sEVs protein lysates. **c** Representative Image showing the proposed mechanism of lncH19 acting as shuttle RNA transferring RBFOX2 inside the EVs. **d** Representative confocal image of RNA in situ assay coupled with immunocytochemistry in the THLE2 treated for 3 h with the CRC-sEVs, lncH19 (red) and RBFOX2 (green). *Scale bar:60 µm*. The results reported in the graphs are the mean ± SD of three independent experiments. Statistical analyses were performed using Ordinary one-way ANOVA *$p < 0.05$, **$p < 0.01$, ***$p < 0.001$. **e** Graphs showing the mean fluorescence intensity (MFI) relative to RBFOX2 (left) and lncH19 (right) of the different conditions

Western Blotting System, cat. n° GERPN2232, Cytiva, Germany) with Chemidoc imaging system (Bio-Rad, Milan, Italy). The images obtained were analysed with the Image Lab software (Bio-Rad).

Confocal fluorescence microscopy

Once removed medium, cells were washed three time with PBS, fixed by adding 4% paraformaldehyde (PFA), permeabilized for 5 min with 0.1% Triton X-100 and, after 1 h of blocking with BSA 3%, incubated for 1 h at room temperature with anti-RBFOX2 primary antibody (1:300 dilution, cat. n° A300-864 A Bethyl Fortis, Montgomery, Texas). After incubation, the unbound primary antibody was removed, and cells were washed with PBS and incubated with DyLight 488 or DyLight 594 secondary antibody (1:500 dilution, Thermo Fisher Scientific, Waltham, MA, USA). Subsequently, unbound secondary antibody was removed, cells were washed with PBS and nuclei were stained with Hoechst (Molecular Probes, cat n° H3570, Life Technologies, Carlsbad, CA, USA). In some cases, cells were stained with Actin Green (1:125 dilution, Thermo Fisher, Waltham, MA, USA) to stain F-actin. Finally, the samples were analysed by confocal fluorescence microscopy (Nikon A1 confocal microscope). Fluorescence analyses were performed using NIS Analysis Software.

RNA in situ hybridisation (RNA Scope)

To visualise the lncH19 localisation in THLE2 treated with CRC-sEVs, RNA in situ protocol was applied as described. After the indicated time-points of treatment, the media were removed, and the cells were washed twice with PBS. Cells were subsequently fixed with 10% Neutral Buffered Formalin (NBF) for 30 min at room temperature, and after fixation were washed twice with PBS and RNAscope® Protease III (1:15 dilution, with PBS) was added for 10 min incubation. Subsequently, cells were washed with PBS and *RNAscope*® Multiplex Fluorescent v2 Assay combined with Immunofluorescence (Cat. n°. 323100) was applied according to the manufacturer's instructions. Fluorescence analyses were performed using NIS Analysis Software.

Bioinformatic analysis

To predict the interactions between lncH19 and its targets in the THLE2, bioinformatic analyses were conducted using DIANA tools [22]. LncH19–miRNA interactions were identified using DIANA-LncBase v.3, and miRPathDB v 2.0 for identifying the miRNAs involved in the EMT process. DIANA-miTED software was used to identify the miRNAs expressed by healthy liver tissue, and all the datasets obtained were intersected using FunRich software. Finally, through the miRPath database, the mRNA targets of the obtained miRNAs were identified.

Statistical analysis

Statistical analysis was performed using GraphPad Prism software (GraphPad software, Inc., La Jolla, CA). Values reported in all graphs are the mean ± standard deviation (SD) of three replicates, unless otherwise stated. The statistical significance of the differences was analysed using Ordinary One-Way ANOVA test. P-values were indicated in the graphs as follows: * $p < 0.05$; ** $p < 0.01$; *** $p < 0.001$ and **** $p < 0.0001$. A p-value ≤ 0.05 was considered significant.

Results

The long non-coding RNA H19 is contained in the CRC-sEVs and is horizontally transferred to the hepatocytes together with RBFOX2

Small EVs have been isolated from CRC cell lines (HCT-116, SW620 and SW480) through differential ultracentrifugation (dUC). SEVs obtained from SW480 and SW620 cell lines have been previously characterized and described by our group [16]; characterisation of HCT-116-derived sEVs is shown in Supplementary Fig. 1a. Here, we firstly investigated the amount of lncH19 in CRC-EVs and, by qRT-PCR we identified higher levels of lncH19 in sEVs compared to relative producing cells (Fig. 2a). Taking inspiration from our recent manuscript that demonstrated the interaction between lncH19 and the splicing factor RBFOX2 [10], we wondered whether RBFOX2 is also loaded inside sEVs. The western blot in Fig. 2b demonstrated, for the first time to our knowledge, that CRC-sEVs contain the RNA-binding protein. To evaluate the EV-mediated co-transport of lncH19 and RBFOX2 (Fig. 2c), we treated THLE2 hepatocytes with CRC-sEVs and three hours after treatment, we performed lncH19 in situ hybridisation combined with immunofluorescence for RBFOX2. As shown by the confocal acquisition (Fig. 2d) and furtherly confirmed by the fluorescence analysis (Fig. 2e), both lncH19 and RBFOX2 increased in recipient cells after sEVs treatment; moreover, the yellow

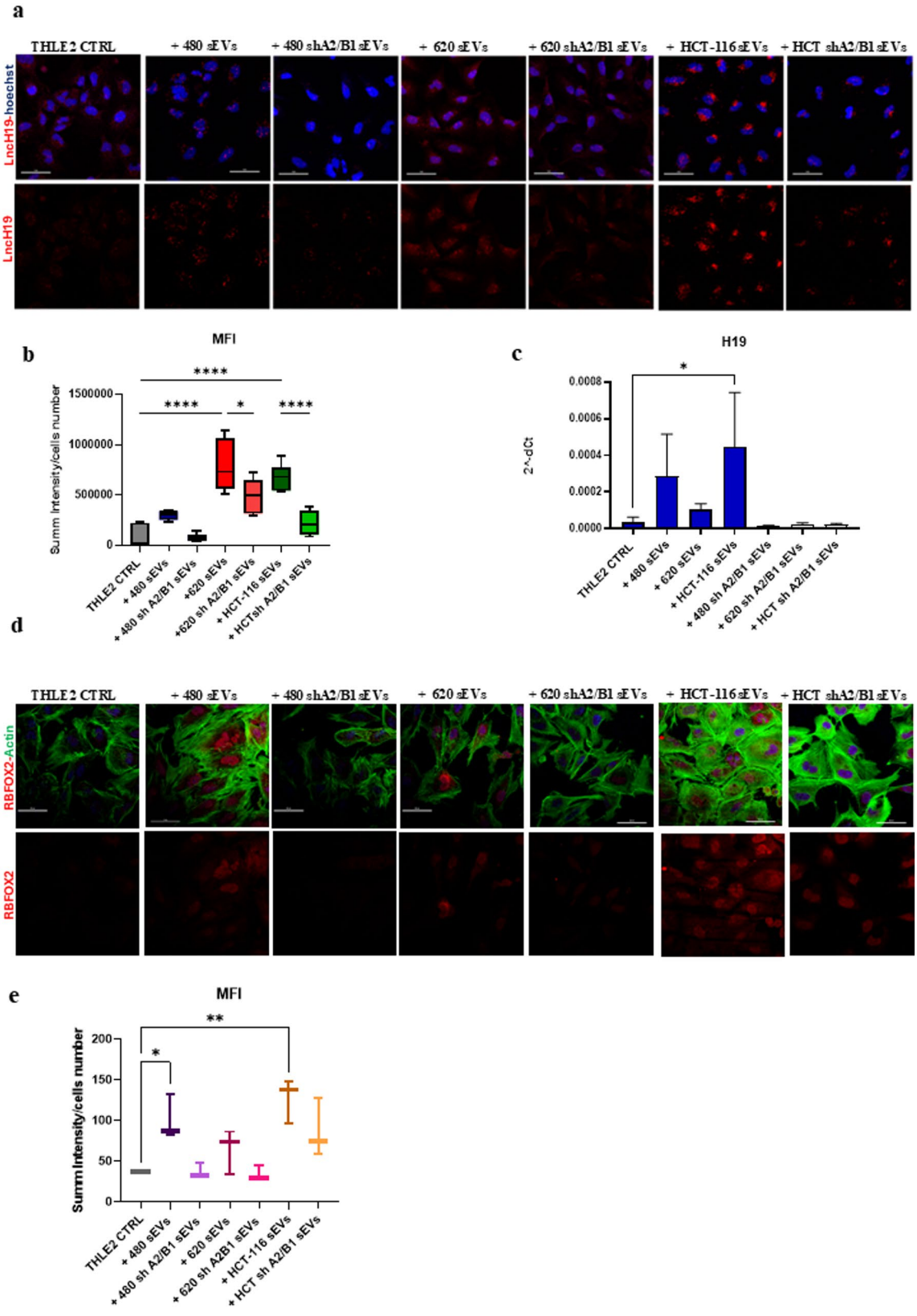

Fig. 3 (See legend on next page.)

(See figure on previous page.)

Fig. 3 **a** Representative confocal micrographs of RNA in situ hybridisation in THLE2 treated for 18 h with the wt-CRC-sEVs and the sh-CRC-sEVs (lncH19 in red, Hoechst in blue). **b** MFI analysis obtained with NIS 1 A analysis software, and (**c**) qRT-PCR showing lncH19 levels in treated cells. (**d**) Representative confocal micrographs of immunocytochemistry for RBFOX2 in the THLE2 treated with wt- and sh- sEVs for 18 h and relative Scale bar: 60 µm (**e**) MFI analysis.The results reported in the graphs are the mean ± SD of three independent experiments. Statistical analyses were performed using Ordinary one-way ANOVA $*p < 0.05$, $**p < 0.01$, $***p < 0.001$

dots indicated co-localisation between the two signals, supporting the hypothesis of a co-transfer lncH19-RBFOX2 from the sEVs to the recipient cells.

hnRNPA2/B1 is crucial for the EV-loading of lncH19 and RBFOX2

As previously demonstrated [23, 24], the lncH19 loading in EVs is mediated by the RNA binding protein hnRNPA2/B1. To investigate to what extent lncH19 loading could be crucial for RBFOX2 transport into vesicles, we silenced hnRNPA2/B1 in CRC cell lines. The efficiency of hnRNPA2/B1 silencing has been validated through qRT-PCR and western blot (Supp. Figure 1b-c). We isolated EVs from CRC cells silenced for hnRNPA2/B1 (from here on sh-CRC-sEVs) and characterised them for EV-specific markers: inclusion of TSG101, HSP70 and absence of the cell-specific marker Calnexin (Supp. Figure 2a). Subsequently, lncH19 levels were evaluated through qRT-PCR. As shown in the Supplementary Fig. 2b, wt-CRC-sEVs contain higher levels of lncH19 compared to their silenced counterparts, thus confirming the role of hnRNPA2/B1 in lncH19 loading, also in CRC-sEVs. We then investigated the presence of RBFOX2 in wt- and sh- sEVs. The western blot in Supplementary Fig. 2c shows that also RBFOX2 levels decreased in EVs obtained from hnRNPA2/B1-silenced cells, thus enforcing our hypothesis of lncH19 as a shuttle for SF in EVs. After characterising and confirming the different molecular cargoes inside the wt-and sh-CRC-sEVs, to investigate the biological activities elicited in the THLE2 hepatocytes, cells were treated for 18 h with the different CRC-sEVs and the lncH19 increase was evaluated through RNA in situ and qRT-PCR.

As shown in Fig. 3a, the treatment with wt-CRC-sEVs induced an increase of lncH19 levels, as confirmed by the fluorescence analysis (Fig. 3b), while this effect was not appreciable after treatment with sh-CRC-sEVs, consistent with the lower levels of the lncRNA in these sEVs. In the same way, immunofluorescence for RBFOX2 in THLE2 cells treated with wt-CRC-EVs highlighted an increase in RBFOX2 signal, more evident in the cytoplasm of treated cells (Fig. 3d-e). This increase is not found in THLE2 cells treated with sh-CRC-EVs. Notably, we did not observe any increase in RBFOX2 mRNA levels in the THLE2 cells treated with the CRC-sEVs (Supp. Figure 2d). This supports the idea that RBFOX2 is directly transferred from the CRC-sEVs to the THLE2 cells, rather than induced at the transcriptional level within the hepatocytes (Fig. 3c).

CRC-sEVs induce AS mechanism in the THLE2

As already mentioned [16], CRC-sEVs induce morphological alteration of the THLE2 promoting EMT, here we wondered if the transported lncH19-RBFOX2 complex might take part in EV-induced transformation. Since the literature described the involvement of RBFOX2 in pro-EMT alternative splicing [7], we focused our further investigation on RBFOX2 target RNAs involved in the definition of the cell shape and morphology: human enabled homolog (ENAH, also known as hMENA), Par-3 family cell polarity regulator (PARD3) and cortactin (CTTN) [25]. It has been demonstrated for these three mRNAs that alternative splicing controls the switch from epithelial to mesenchymal isoforms. In particular, the mRNA of ENAH is described to be subjected to the skipping of exons 6 an 11 A during the EMT process [26], while for CTTN mRNA, the inclusion of exon 11 is associated with EMT and increased aggressiveness in colon cancer forms [27]. Finally, PARD3 mRNA undergoes exon 18 skipping during EMT. By designing exon-specific primers, we evaluated the expression of AS variants as well as the common gene isoforms. As shown by the qRT-PCR in Fig. 4a, left panel, the common transcripts do not show an increase in the THLE2 cells treated with the CRC-sEVs, except for PARD3. In contrast, the AS variants seem to be affected by the treatment with the CRC-sEVs. In particular, only wt-CRC sEVs induced the skipping of exons 6 of ENAH, the inclusion of exon 11 of CTTN, and the skipping of exon 18 of PARD3 this mainly appreciable with sEVs isolated from HCT-116 cells (Fig. 4b). Overall, the data here showed indicated that wt-CRC-EVs treatment induced AS in hepatocytes, favouring RBFOX2 mediated mesenchymal isoforms. Notably, sEVs containing a lower amount of both molecules lncH19 and RBFOX2, did not promote specific AS, except for ENAH 11a exclusion, which was equally promoted by all vesicles.

EV-H19 acts as a miRNA sponge in hepatocytes

If RBFOX2 transport can justify the alternative splicing of its targets, it is still interesting to note that wt-CRC_EVs also induced the increase of PARD3 transcription. To shed light on this increase, we focused on the possible sponge activity of lncH19. Using different Bioinformatic tools (Diana-LncBase v.3, DIANA-miTED and miRPathDB v.20), we performed an analysis evaluating all the miRNAs sponged by lncH19, expressed in healthy liver and involved in the EMT process (Fig. 5a). By Funrich

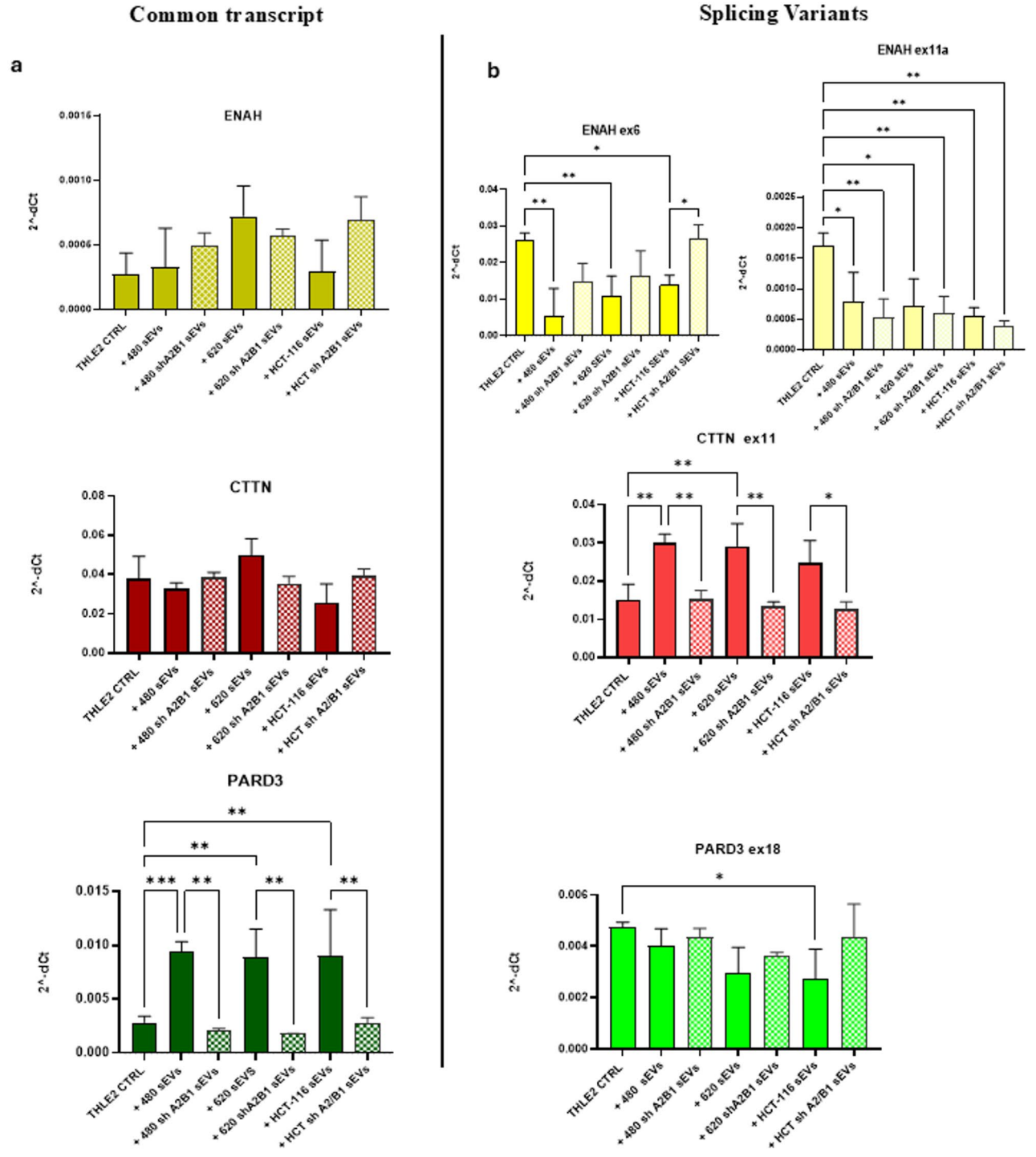

Fig. 4 **a** qRT-PCR and (**b**) exon-specific qRT-PCR showing the expression levels of ENAH, CTTN and PARD3 genes in THLE2 treated with the wt- and sh-CRC-sEVs

analysis, we intersected three datasets and identified eleven miRNAs, among these 4 share PARD3 mRNA as a common target (Fig. 5b). To validate the direct action of lncH19 on PARD3 expression, we induced lncH19 overexpression in the hepatocytes and as shown in Fig. 5, PARD3 mRNA increase in the THLE2 overexpressing lncH19 (Fig. 5c-d). Although we did not validate the direct role of identified miRNA in this process, the data here obtained indicated that lncH19 and RBFOX2 can act synergistically on AS and transcriptional regulation affecting gene expression in hepatocytes.

a

Query	Database	Output
miRNAs sponged by lncH19	DIANA – LncBase v.3	160
miRNAs involved in EMT	mirPATH database	108
miRNA expressed by healthy liver tissue	DIANA-miTED	2636

b

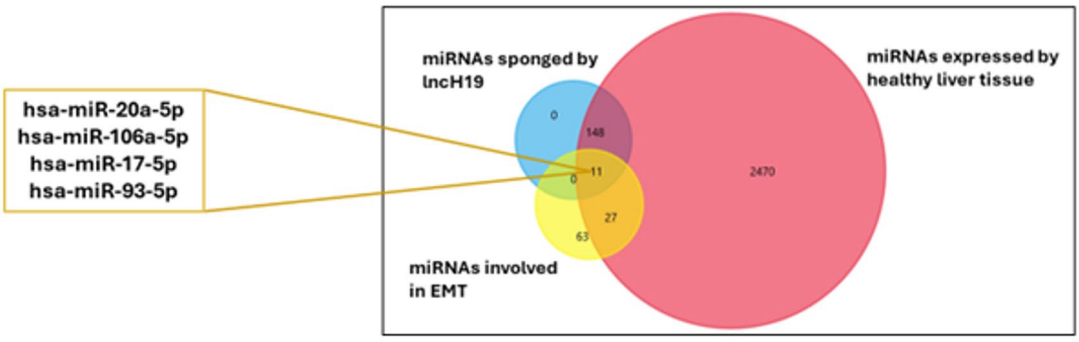

c

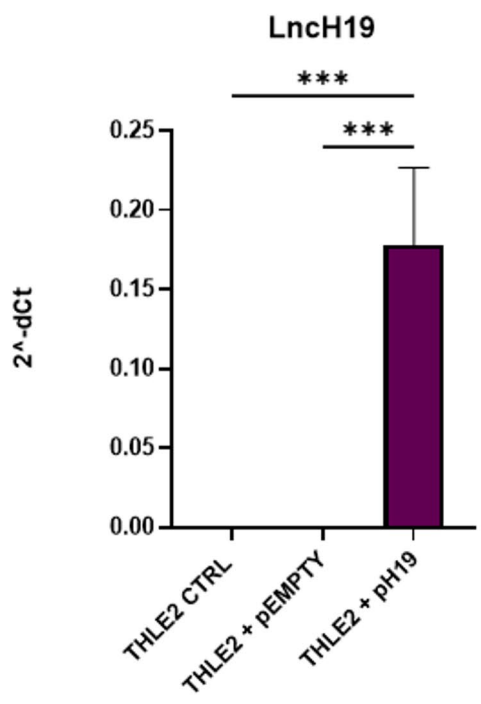

d

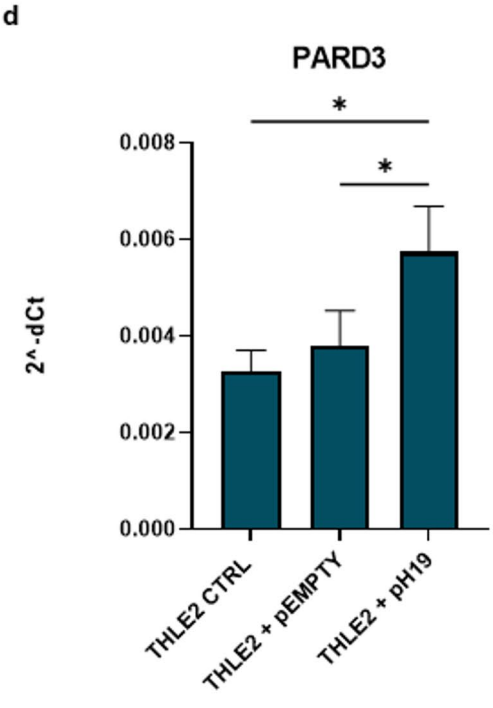

Fig. 5 **a** Table showing the different miRNAs identified in the three different analyses (sponged by lncH19, involved in EMT and expressed by healthy liver tissue). **b** Venn Diagram from FunRich analysis of data obtained by the three indicated datasets. The square in figure indicates 4 from 11 miRNAs targeting PARD3 mRNA **c** qRT-PCR confirming the over-expression of lncH19 in the THLE2 and (**d**) the increase of PARD3 mRNA in the H19-overexpressing hepatocytes

Discussion

Horizontal RNA transfer mediated by EVs has emerged over the past decade as an engaging area of investigation, attracting significant attention from both basic and translational research. Fundamental studies have focused on elucidating the mechanisms of RNA loading into EVs, the selective packaging of specific RNA species, and the functional impact of transferred RNA on recipient cells. Concurrently, applied research has explored the potential of intra-vesicular RNA as a biomarker for disease states and as a novel therapeutic modality, highlighting its dual role in diagnostics and targeted interventions. This fascinating field is growing in parallel with the knowledge about the role and mechanism of action of long non-coding RNAs.Our investigations were among the first to identify the presence of lncH19 within EVs [17]. Following our initial discovery, several research groups also reported the detection of various lncRNAs in EVs, paving the way for investigations into their loading mechanisms and functional roles in recipient cells.The molecular process of ncRNAs packaging inside the EVs has gained increasingly interest, and even though the complex detail of such process is still not completely understood, new key molecular players have been identified in the recent years [28]. For example, Y-box protein 1 (YBX1) has been described to regulate miRNA-secretion in EVs released by HEK293T cells [29]. Also, SYNCRIP, another RNA-binding protein, has been described by Santangelo et al. to be crucial for the delivery of miRNAs inside the EVs [29, 30].

Poorly investigated is the mechanism governing lncRNA loading in EVs however. Despite the scarce evidence, two different papers identified the RNA-binding protein hnRNPA2B1 as a key mediator responsible for incorporating lncH19 into vesicular cargo [23, 31].

In this manuscript we confirmed the pivotal role of hnRNPA2/B1 in the loading of lncH19, showing as the silencing of the RNA binding protein, strongly affects lncH19 levels only inside the EVs. Moreover, by strategically silencing hnRNPA2/B1 to regulate lncH19 loading into extracellular vesicles, we uncovered a previously unrecognized role of lncH19 as a molecular hub, orchestrating the co-transport of associated proteins. These studies further explored and characterised the mechanisms underlying the RNAs' packaging and their subsequent delivery to recipient cells. Notably, the predominant functional activity documented for these transferred lncRNAs pertains to their role as competitive endogenous RNAs, acting as molecular sponges for microRNAs. LncRNAs are in fact implicated in the regulation of different cellular functions in both physiological and pathological conditions [32]. Their action is mostly studied for their ability to establish interaction with RNA, DNA and proteins [33]. They can act as decoy for transcription factors, guiding chromatin modifications, scaffold for different multimolecular complexes, and sponging miRNAs thus ultimately leading to alteration in gene expression [34].

More than 90% introns-containing genes are subjected to AS in humans [35]. This process is generally highly regulated, and recent evidence has highlighted how the aberrant AS is associated with pathological conditions, such as cancer initiation and progression [36], However, the possible role of lncRNAs in this finely regulated process is still underestimated and only partially investigated [37]. Moreover, here we suggest a more complex scenario than previously described, drawing attention to a phenomenon that is increasingly evident: lncRNAs rarely act in isolation. Instead, they often serve as platforms for multimolecular complexes including RNABP and other RNA species.

Building on our recent data demonstrating the physical interaction between lncH19 and RBFOX2 in CRC cells [10], here we demonstrate that both molecules are loaded into EVs and delivered into healthy hepatocytes. Although the sEVs treatments induce only a slight increase of RBFOX2 protein levels in hepatocytes, it is sufficient to move the splicing pattern to pro-EMT isoforms. This lets us hypothesise that delivered RBFOX2, probably in cooperation with lncH19, recognise different splicing sites. However, we cannot exclude that other molecular mediators, transported by CRC-EVs, cooperate in this sense, as suggested by the data obtained on ENAH 11a exon. This, in fact, is always excluded by EV treatment regardless EVs' origin and lncH19/RBFOX2 content. Notably, the increase of RBFOX2 in hepatocytes treated with CRC-sEVs is mainly appreciable in the cytoplasm, this lets that EVs may be involved in the mechanisms inducing cytoplasmic splicing [38]. Also, this molecular complex may directly act in the cellular nucleus. Our evidence, though indirectly, also enforces the experimental theory regarding the possibility of EVs to deliver their molecular cargo inside nuclear compartment of recipient cells, where these AS related mechanism induced by EV-H19 probably take place. In fact, one of the biggest questions in EV-research field regarded the possibility of small EVs to deliver their content without undergoing lysosomal degradation [39]. In some studies, it has been reported that a small fraction of the EVs can translocate inside the nucleoplasmic reticulum, reaching a deeper localization near the nucleolus. The research group led by Lorico has in fact demonstrated that Rab7 + late endosomes enter type II nuclear envelope invagination (NEI), formed by the inner and outer nuclear membranes (INM and ONM respectively) [40]. Mechanistically, the fusion of endocytosed EVs with the membrane of late endosomes inside NEI will lead to a release of the EV content, facilitating their transfer into

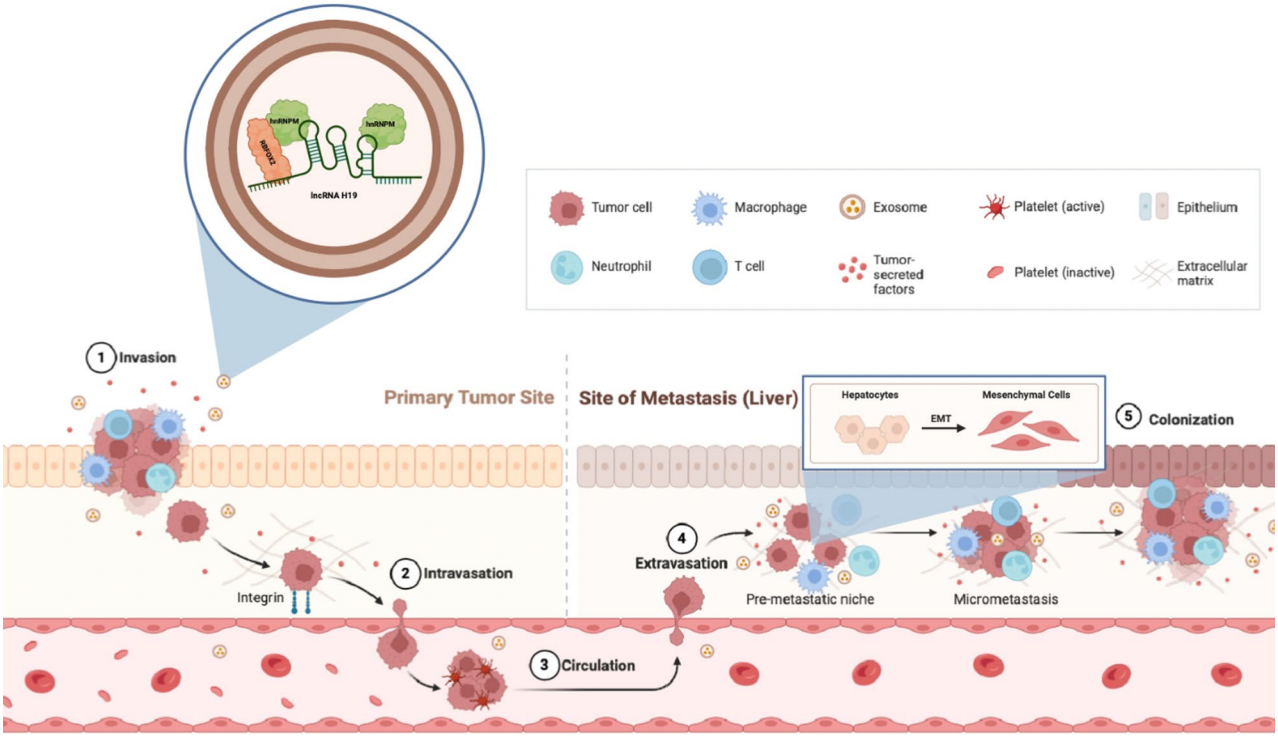

Fig. 6 Schematic representation of the proposed mechanism: LncH19 and RbFOX2 transported by CRC-sEVs reach the distant site of future metastasis (liver), and affect the PMN through dysregulating key molecular processes such AS

the nucleoplasm through the nuclear pores [41]. Because of the appearance of late endosomes entering the nucleoplasmic reticulum resembles a sword, these double-organelle structures have been called "Spathasomes" [42].

Increasing evidence supports the role of TD_sEVs released by primary tumour in the promotion of the PMN formation, also in distant sites [43]. In the liver, CRC-sEVs have been shown to enforce this pre-metastatic environment, regulating different biological processes, such as Immune regulation, angiogenesis, EMT, fibrosis [44, 45]. While most of the studies have been focusing on the effects of CRC-sEVs on the non-parenchymal component of the liver, such as hepatic stellate cells and Kupffer cells, data regarding their effect on hepatocytes in the early stage of PMN establishment is still lacking [46, 47]. Although recent studies have demonstrated that CRC-sEVs promote EMT in hepatocytes [16], the molecular mechanisms underlying this process are clear only partially. In this study, we provided the first evidence that CRC-sEVs can affect gene expression in hepatocytes by dysregulating AS, ultimately leading to the formation of mesenchymal transcript variants. In this perspective, the increase in PARD3 levels and the subsequent pro-mesenchymal splicing present a scenario in which different macromolecules contribute to the creation of the same phenotype which in this context is the definition of a niche favourable to the metastasis process (Fig. 6).

Overall, our data represent one of the first milestones to shed light on a previously underestimated biological process affected by TD_sEVs, such as Alternative Splicing, and how tackling this mechanism can lead to a better understanding of the PMN formation and eventually to develop new therapeutic strategies to prevent metastases formation in CRC patients. Even though further studies still need to be conducted to confirm the role of lncH19 as a molecular shuttle in EVs and the association of AS induction with the establishment of a pro-metastatic microenvironment, the data reported highlight H19 in a previously underestimated molecular process.

Limitations of the study

In the present study, we demonstrated that CRC-sEVs can affect AS in recipient cells. In particular, we focused on the role of lncH19 and RBFOX2 and how this molecular complex promotes AS shifting RBFOX2 target mRNAs towards their "mesenchymal counterpart". Unfortunately, we couldn't evaluate the protein relative to these mRNAs, due to the lack of specific antibodies, moreover a deeper investigation is required to confirm the binding between lncH19 and RBFOX2 inside CRC-sEVs, however we believe that this first data may give a boost to the study of

the horizontal transfer of lncRNA mediated by extracellular vesicles.

Supplementary Information

The online version contains supplementary material available at https://doi.org/10.1186/s12964-026-02738-x.

Supplementary Material 1.

Supplementary Material 2.

Supplementary Material 3.

Supplementary Material 4.

Supplementary Material 5.

Acknowledgements
Thanks to Prof Maria Magdalena Barreca for her contribution during the experimental design phase and for the ongoing constructive dialogue. The authors would like to thank the ATeN Center at the University of Palermo for the cell sorting of the sh-CRC_cell lines.

Authors' contributions
ACon, ML: Conceptualization; ACon and ML: Project administration; ML, CZ, DA, ACor: Investigation and Methodology; Data curation: ACon and ML; Writing original draft: ML and ACon; SF and RA: Visualization and editing; ACon: Funding acquisition; AC and RA: Supervision.

Funding
This research was funded by AIRC under the MFAG 2017 program—ID. 19982—P.I. Alice Conigliaro and by a grant from the University of Palermo to Alice Conigliaro Bando EUROSTART 2025 project title: "Il trasferimento orizzontale dei long non coding RNA ed il loro ruolo nella formazione della nicchia pre-metastatica".
Marco Loria was supported by the PhD program in "Oncologia e Chirurgia Sperimentale", University of Palermo. Aurora Cordaro and Denise Anello are PhD students in "Biomedicine, Neuroscience and Advanced Diagnostics", XXXVIII and XXXIX cycle respectively, University of Palermo.

Data availability
No datasets were generated or analysed during the current study.

Declarations

Competing interests
The authors declare no competing interests.

Received: 6 November 2025 / Accepted: 7 February 2026
Published online: 17 February 2026

References

1. Marabti EE, Younis I. The cancer spliceome: reprograming of alternative splicing in cancer. Front Media SA. 2018. https://doi.org/10.3389/fmolb.2018.00080.
2. Bonner EA, Lee SC. Therapeutic Targeting of RNA Splicing in Cancer. Multidisciplinary Digital Publishing Institute (MDPI). 2023. https://doi.org/10.3390/genes14071378.
3. Zhang Y, Qian J, Gu C, Yang Y. Alternative splicing and cancer: a systematic review. Springer Nature; 2021. https://doi.org/10.1038/s41392-021-00486-7.
4. Liu Z, Rabadan R. Computing the Role of Alternative Splicing in Cancer. Cell Press. 2021. https://doi.org/10.1016/j.trecan.2020.12.015.
5. Xiong Y, et al Profiles of alternative splicing in colorectal cancer and their clinical significance: A study based on large-scale sequencing data. EBioMedicine. 2018;36:183–95. https://doi.org/10.1016/j.ebiom.2018.09.021.
6. Zong Z, Li H, Yi C, Ying H, Zhu Z, Wang H. Genome-wide profiling of prognostic alternative splicing signature in colorectal cancer. Front Oncol. 2018;8. https://doi.org/10.3389/fonc.2018.00537.
7. Venables JP, et al RBFOX2 is an important regulator of mesenchymal Tissue-Specific splicing in both normal and cancer tissues. Mol Cell Biol. 2013;33(2):396–405. https://doi.org/10.1128/mcb.01174-12.
8. Braeutigam C, Rago L, Rolke A, Waldmeier L, Christofori G, Winter J The RNA-binding protein Rbfox2: An essential regulator of EMT-driven alternative splicing and a mediator of cellular invasion. Oncogene. 2014;33(9):1082–92. https://doi.org/10.1038/onc.2013.50.
9. Mochizuki Y, et al Alternative microexon splicing by RBFOX2 and PTBP1 is associated with metastasis in colorectal cancer. Int J Cancer. 2021;149(10):1787–800. https://doi.org/10.1002/ijc.33758.
10. Cordaro A, et al. Regulatory role of lncH19 in RAC1 alternative splicing: implication for RAC1B expression in colorectal cancer. J Experimental Clin Cancer Res. 2024;43(1). https://doi.org/10.1186/s13046-024-03139-z.
11. Zhou H et al. Colorectal liver metastasis: molecular mechanism and interventional therapy. Springer Nature; 2022. https://doi.org/10.1038/s41392-022-00922-2.
12. Haggar FA, Boushey RP. Colorectal cancer epidemiology: Incidence, mortality, survival, and risk factors. Clin Colon Rectal Surg. 2009;22(4):191–7. https://doi.org/10.1055/s-0029-1242458.
13. Chandra R et al. The colorectal cancer tumor microenvironment and its impact on liver and lung metastasis. MDPI; 2021. https://doi.org/10.3390/cancers13246206.
14. Yao H, et al. Extracellular vesicle-packaged LncRNA from cancer-associated fibroblasts promotes immune evasion by downregulating HLA-A in pancreatic cancer. J Extracell Vesicles. 2024;13(7). https://doi.org/10.1002/jev2.12484.
15. Ciardiello C, Migliorino R, Leone A, Budillon A. Large extracellular vesicles: Size matters in tumor progression. Elsevier Ltd.; 2020. https://doi.org/10.1016/j.cytogfr.2019.12.007.
16. Pucci M, et al. Colorectal cancer-derived small extracellular vesicles induce TGFβ1-mediated epithelial to mesenchymal transition of hepatocytes. Cancer Cell Int. 2023;23(1). https://doi.org/10.1186/s12935-023-02916-8.
17. Conigliaro A, et al. CD90 + liver cancer cells modulate endothelial cell phenotype through the release of exosomes containing H19 LncRNA. Mol Cancer. Aug. 2015;14(1). https://doi.org/10.1186/s12943-015-0426-x.
18. Tao S, et al. Extracellular vesicles released by hypoxia-induced tumor-associated fibroblasts impart chemoresistance to breast cancer cells via long noncoding RNA H19 delivery. FASEB J. 2024;38(2). https://doi.org/10.1096/fj.202300203R.
19. Zhao H, Jiang R, Zhang C, Feng Z, Wang X. LncRNA H19-rich extracellular vesicles derived from gastric cancer stem cells facilitate tumorigenicity and metastasis via mediating intratumor communication network. J Transl Med. 2023;21(1). https://doi.org/10.1186/s12967-023-04055-0.
20. Schillaci O, et al. Exosomes from metastatic cancer cells transfer amoeboid phenotype to non-metastatic cells and increase endothelial permeability: their emerging role in tumor heterogeneity. Sci Rep. 2017;7(1). https://doi.org/10.1038/s41598-017-05002-y.
21. Welsh JA, et al. Minimal information for studies of extracellular vesicles (MISEV2023): from basic to advanced approaches. J Extracell Vesicles. 2024;13(2). https://doi.org/10.1002/jev2.12404.
22. Rincón-Riveros A, Morales D, Rodríguez JA, Villegas VE, López-Kleine L. Bioinformatic tools for the analysis and prediction of ncrna interactions. MDPI; 2021. https://doi.org/10.3390/ijms222111397.
23. Song Y, Guo N, Zi F, Zheng J, Cheng J. lncRNA H19 plays a role in multiple myeloma via interacting with hnRNPA2B1 to stabilize BET proteins by targeting osteoclasts and osteoblasts, Int Immunopharmaco. 2024;142. https://doi.org/10.1016/j.intimp.2024.113080.
24. Tao SC, Huang JY, Li ZX, Zhan S, Guo SC. Small extracellular vesicles with LncRNA H19'overload': YAP regulation as a tendon repair therapeutic tactic. iScience. 2021;24(3). https://doi.org/10.1016/j.isci.2021.102200.
25. Gardina PJ, et al. Alternative splicing and differential gene expression in colon cancer detected by a whole genome exon array. BMC Genomics. 2006;7. https://doi.org/10.1186/1471-2164-7-325.
26. Di Modugno F, et al Splicing program of human MENA produces a previously undescribed isoform associated with invasive, mesenchymal-like breast tumors. Proc Natl Acad Sci USA. 2012;109(47):19280–5. https://doi.org/10.1073/pnas.1214394109.
27. Verma SK, et al Feb., RBFOX2 is required for establishing RNA regulatory networks essential for heart development. Nucleic Acids Res. 2022;50(4):2270–86. https://doi.org/10.1093/nar/gkac055.
28. Yang S, Li X. Recent advances in extracellular vesicles enriched with noncoding RNAs related to cancers. Chongqing University; 2018. https://doi.org/10.1016/j.gendis.2017.12.001.

29. Corrado C, Barreca MM, Zichittella C, Alessandro R, Conigliaro A. Molecular mediators of rna loading into extracellular vesicles. MDPI; 2021. https://doi.org/10.3390/cells10123355.
30. Santangelo L, et al The RNA-Binding protein SYNCRIP is a component of the hepatocyte Exosomal machinery controlling MicroRNA sorting. Cell Rep. 2016;17(3):799–808. https://doi.org/10.1016/j.celrep.2016.09.031.
31. Zhang Y, et al. Long non-coding RNA H19 promotes colorectal cancer metastasis via binding to hnRNPA2B1. J Experimental Clin Cancer Res. 2020;39(1). https://doi.org/10.1186/s13046-020-01619-6.
32. Sebastian-Delacruz M, Gonzalez-Moro I, Olazagoitia-Garmendia A, Castellanos-Rubio A, Santin I. non-coding RNA the role of LncRNAs in gene expression regulation through mRNA stabilization. 2021. https://doi.org/10.3390/ncrna.
33. He RZ, Luo DX, Mo YY. Emerging roles of lncRNAs in the post-transcriptional regulation in cancer. Chongqing University; 2019. https://doi.org/10.1016/j.gendis.2019.01.003.
34. Zhang X et al. Mechanisms and functions of long non-coding RNAs at multiple regulatory levels. MDPI AG; 2019. https://doi.org/10.3390/ijms20225573.
35. Wang X, et al. Mechanisms of non-coding RNA-modulated alternative splicing in cancer. Taylor Francis Ltd. 2022. https://doi.org/10.1080/15476286.2022.2062846.
36. Gonzalez I, et al A LncRNA regulates alternative splicing via establishment of a splicing-specific chromatin signature. Nat Struct Mol Biol. 2015;22(5):370–6. https://doi.org/10.1038/nsmb.3005.
37. Pisignano G, Ladomery M. Epigenetic regulation of alternative splicing: how Lncrnas tailor the message. MDPI AG. 2021. https://doi.org/10.3390/ncrna7010021.
38. Buckley PT, Khaladkar M, Kim J, Eberwine J. Cytoplasmic intron retention, function, splicing, and the Sentinel RNA hypothesis. Mar. 2014. https://doi.org/10.1002/wrna.1203.
39. Lorico A, Santos MF, Karbanová J, Corbeil D. Extracellular membrane particles en route to the nucleus – exploring the VOR complex. Portland Press Ltd; 2025. https://doi.org/10.1042/BST20253005.
40. Malhas A, Goulbourne C, Vaux DJ. The nucleoplasmic reticulum: form and function. Jun. 2011. https://doi.org/10.1016/j.tcb.2011.03.008.
41. Santos MF, et al. Itraconazole inhibits nuclear delivery of extracellular vesicle cargo by disrupting the entry of late endosomes into the nucleoplasmic reticulum. J Extracell Vesicles. 2021;10(10). https://doi.org/10.1002/jev2.12132.
42. Rappa G et al. Nuclear transport of cancer extracellular vesicle-derived biomaterials through nuclear envelope invagination-associated late endosomes. 2017. Available: https://www.impactjournals.com/oncotarget/.
43. Dong Q, Liu X, Cheng K, Sheng J, Kong J, Liu T. Pre-metastatic Niche Formation in Different Organs Induced by Tumor Extracellular Vesicles. Frontiers Media S.A. 2021. https://doi.org/10.3389/fcell.2021.733627.
44. Si G, Chen X, Li Y, Yuan X. Exosomes promote pre-metastatic niche formation in colorectal cancer. Elsevier Ltd; 2024. https://doi.org/10.1016/j.heliyon.2024.e27572.
45. Yang X et al. Colorectal cancer-derived extracellular vesicles induce liver premetastatic immunosuppressive niche formation to promote tumor early liver metastasis. Springer Nature; 2023. https://doi.org/10.1038/s41392-023-01384-w.
46. Zhao S et al. Jan., Highly-metastatic colorectal cancer cell released miR-181a-5p-rich extracellular vesicles promote liver metastasis by activating hepatic stellate cells and remodelling the tumour microenvironment. J Extracell Vesicles. 2022;11(1). https://doi.org/10.1002/jev2.12186.
47. Costa-Silva B et al. Jun., Pancreatic cancer exosomes initiate pre-metastatic niche formation in the liver. Nat Cell Biol. 2015;17(6):816–826. https://doi.org/10.1038/ncb3169.

Publisher's Note